

Number 33
July 2008

SWISS NEUTRON NEWS



Walter E. Fischer



Schweizerische Gesellschaft für Neutronenstreuung
Société Suisse pour la Diffusion des Neutrons
Swiss Neutron Scattering Society

EDITORIAL:

Editor: Swiss Neutron Scattering Society

Board for the Period June 2007 – June 2010:

President: Dr. P. Allenspach peter.allenspach@psi.ch

Board Members: Prof. Dr. S. Decurtins silvio.decurtins@iac.unibe.ch
Prof. Dr. B. Schönfeld schoenfeld@iap.phys.ethz.ch

Secretary: Dr. S. Janssen stefan.janssen@psi.ch

Honorary Members: Prof. Dr. W. Hälg, ETH Zürich
Prof. Dr. K.A. Müller, IBM Rüschlikon and Univ. Zürich
Prof. Dr. A. Furrer, ETH Zürich and Paul Scherrer Institut

Auditors: Dr. K. Krämer, University of Berne
N.N.

Address: Sekretariat SGN/SSDN
Paul Scherrer Institut
bldg. WLGA/002
5232 Villigen PSI, Switzerland
phone: +41-(0)56 - 310 4666
fax: +41-(0)56 - 310 3294
www: <http://sgn.web.psi.ch>

Bank Account: Postfinance: 50-70723-6
BIC: POFICHBE
IBAN: CH39 0900 0000 5007 0723 6

Printing: Paul Scherrer Institut

Circulation: 2150, 2 numbers per year

Copyright: SGN/SSDN and the respective authors

ON THE COVER:

Walter E. Fischer, the pioneer in establishing the spallation neutron source SINQ at PSI Viligen, passed away on March 17, 2008 (see the obituary notice written by Albert Furrer in this issue). The Swiss Neutron Scattering Society and all Walter's friends and colleagues will never forget him.

Contents

- 2** The President's Page
- 4** In-situ Deformation under Neutrons as a Tool to Uncover the Plasticity Mechanisms of Nanostructured Cu-Nb-Based Wires
- 10** Neutron Scattering Spectroscopy of Relaxor Ferroelectrics
- 18** The First "joint X+N" Proposals Round for Powder Diffraction Experiments at PSI
- 20** Walter E. Fischer (1939-2008)
- 22** Joël F. Mesot New Director of the Paul Scherrer Institut
- 23** SGN Financial Report 2007
- 24** Zuoz 2008 – announcement
- 25** Announcements
- 26** Conferences and Workshops 2008
- 29** Conferences and Workshops 2009

The President's Page



DEAR MEMBERS

The EU-FP7 ESS preparatory phase (ESS-PP) has been running since April 1, 2008. This project should update and collate existing information about ESS but also add some new aspects such as location, legal and governance issues as well as assessments of the radioactive inventory and decommissioning. While all this work has to be done within a certain time during the process towards the realization of ESS, non of these tasks must delay a decision on ESS. However, presently we are so to speak victim of our success: With three governments (Spanish, Swedish and Hungarian) eager to host ESS, the creation of a consortium of countries is hampered. Most European countries will participate in the construction and

operation of ESS, but for them, the location is of minor importance and they are not yet willing to commit themselves to one of the three projects. The paramount importance of the location on the decision of ESS has been recognized by EU and ESFRI (European Strategy Forum for Research Infrastructures). Together with the fact that ESS-PP cannot take a decision on the location this led to the creation of the ESFRI Expert Working group on ESS siting (EWESS) headed by Paul Zinsli, vice director of the Swiss Secretary of State for Education and Research. A questionnaire was set up for the three official sites which have all been answered and been sent back at the end of April. In July, an expert group called SRG consisting of three experts (individually accepted by each of the sites) and Peter Tindemans as scientific secretary will visit each site for two days. Their duty will be to assess the answers to the questionnaire and particularly the locations and to report back on this to EWESS by mid September. Hopefully this report will initiate consortia negotiations from governments of non-site countries with their then favorite ESS project.

What about the Swiss neutron users and the choice of their ESS site? Does it matter? I strongly believe that the location is really a minor concern for users. The major issue for them is the realization of ESS. Often, acces-

sibility is brought into the discussion. This is certainly a question of quality of scientific life. How then does the accessibility of the three sites compare if I would have to start an experiment – say this September 16 at 9 am in Bilbao, Lund or Debrecen, respectively? Anyhow, I would have to travel the day before and would have to take a flight at Zurich airport at 17:40 for Debrecen, 19:00 for Bilbao and 20:00 for Lund. Is this difference decisive? Similar time differences are observed all over Europe with the only obvious difference close to the respective sites (see Figure).

SINQ has re-started operation on May 13, slightly delayed due to the installation of the intermediate heavy water loop and the re-purification of the heavy water in the moderator tank. With these measures we will avoid similar problems in the future and are back within a few percent of the original neutron flux. Many thanks to the SINQ team for their excellent work and to the PSI directorate for its support.

Peter Allenspach



Figure: Departure time before start of an experiment (September 16, at 9 o'clock) at one of the three ESS sites. Itineraries taken from www.swoodoo.de on May 26. Exercise conditions: For travels on September 16 arrival at Copenhagen airport before 8:00. For September 15 arrivals at Budapest airport before 22:00 (due to the car trip of about 2 hours to Debrecen).

In-situ Deformation under Neutrons as a Tool to Uncover the Plasticity Mechanisms of Nanostructured Cu-Nb-Based Wires

L. Thilly¹, V. Vidal², S. Van Petegem³, U. Stuhr⁴, F. Lecouturier⁵,
P.-O. Renault¹, H. Van Swygenhoven³

¹PHYMAT, Université de Poitiers, 86960 Futuroscope, France

²CROMeP, ENSTIMAC, Campus Jarlard, 81013 Albi, France

³Paul Scherrer Institut, Villigen PSI, 5232 Switzerland

⁴Laboratory for Neutron Scattering, ETH Zürich & Paul Scherrer Institut, Villigen PSI, 5232 Switzerland

⁵Laboratoire National des Champs Magnétiques Pulsés, CNRS-UPS-INSA, 143 avenue de Ranguéil,
31400 Toulouse, France

High strength Cu-Nb-based wires for high field pulsed magnets composed of a Cu matrix embedding Nb nanofilaments or nanotubes are studied using in-situ tensile testing during neutron diffraction at POLDI, SINQ. The evolution of lattice strains during deformation reveals the phase-specific elasto-plastic regimes, uncovering the effect of size on the strengthening mechanisms in complex nanostructured materials.

INTRODUCTION

The growing need for multi-functional materials and the continuous miniaturization of devices lead to the development of new composite materials with grains in the nanometer range and/or nanosized phases. The mechanical properties of each phase of these

nanocomposites are then strongly influenced by the high interface to volume ratio of the grains and their plasticity, dislocation-mediated at large grain size, is modified by so-called “size effects” [1]. Moreover, the combination of different phases with different microstructure dimensions leads to complex co-deformation behaviour, which understanding and control are crucial for the nanocomposites applications. An example of challenging application is the development of reinforced conductors for the winding of high pulsed magnets that requires materials with high electrical conductivity and high strength [2]. To obtain fields over 80T, yield stress of the order of 2 GPa (at 77K) is needed: only Cu-Nb-based nanocomposite wires can reasonably exhibit low electrical resistivity with such elastic limit [3, 4]. Nevertheless, their fabrication is limited by the understanding of the

mechanical properties of each phase and their combination.

The effect of microstructure refinement on the mechanical properties of Cu/Nb nanocomposites, composed of a Cu matrix embedding Nb nanofilaments, was studied using in-situ deformation in a Transmission Electron Microscope (TEM) [5]: a reduction of dislocation activity was observed in the Cu matrix confined at the nanometre scale, a mechanism that has also been reported for nanolayered composites [3]. Therefore, the strengthening of the Cu matrix was modeled by an Orowan-type size dependence of the Cu yield stress, $\sigma_y(\text{Cu})$, proportional to $(1/d_{\text{Cu}})\ln(d_{\text{Cu}})$, where d_{Cu} is the Cu grain size [3–5]. For the Nb nanofilaments a whisker-type behavior was observed that is described by an exponential dependence of the yield stress on the filaments diameter d_{Nb} ($\sigma_y(\text{Nb}) \propto \exp(-d_{\text{Nb}})$), approaching the theoretical strength for $d_{\text{Nb}} < 100 \text{ nm}$ [4].

The previous phase-specific strengthening scaling laws can be successfully used to predict, with a Rule Of Mixtures (ROM), the nanocomposites mechanical properties but the details of the co-deformation mechanism remain unanswered.

Thanks to the high penetration depth of thermal neutrons and the crystallographic selectivity of diffraction, in-situ deformation under neutrons was performed with the objectives to reveal the phase-specific elasto-plastic behaviour of Cu-Nb-based wires and confirm the strengthening mechanisms.

MATERIALS CHARACTERISTICS

The wires are produced by Severe Plastic Deformation (SPD) via the Accumulative Drawing and Bundling (ADB) process described in detail in ref 3. The obtained conductors are composed of a pure copper matrix embedding N^n ($N=55$ or 85 , $n \leq 4$) Nb nanofilaments (Cu/Nb wires) or nanotubes (Cu/Nb/

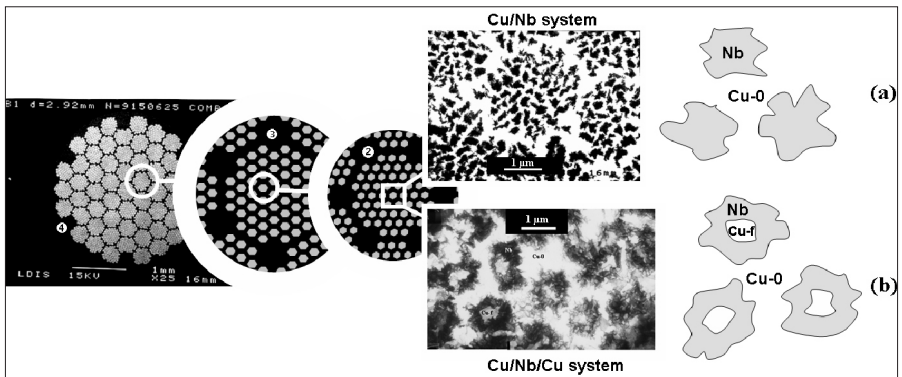


Figure 1: Successive micrographs showing cross-sections of the multiscale structure of the Cu/Nb and Cu/Nb/Cu conductors. (a) SEM micrograph and schematic of Cu/Nb wire containing $N=55^4$ Nb nanofilaments, at diameter $d=2.9 \text{ mm}$. (b) TEM micrograph and schematic of Cu/Nb/Cu wire containing $N=85^3$ Nb nanotubes, at diameter $d=1.5 \text{ mm}$.

Table 1: microstructure characteristics (average dimensions) of two wires from the Cu/Nb/Cu and Cu/Nb systems at similar total diameter $d = 1.5$ mm. **Bold** dimensions for the Cu- i channels define the “fine-Cu” channels.

system	N^n	t_{Nb}, d_{Nb} (nm)	d_{Cu-f} (nm)	d_{Cu-0} (nm)	d_{Cu-1} (nm)	d_{Cu-2} (μ m)	d_{Cu-3} (μ m)	d_{Cu-4} (μ m)	UTS (MPa)
Cu/Nb/Cu	85 ³	263	388	277	1070	11.6	63	---	880
Cu/Nb	55 ⁴	267	---	45	149	1.3	10.7	47	1100

N^n : number of nanotubes or nanofilaments; t_{Nb} : thickness of nanotubes; d_{Nb} : diameter of nanofilaments; d_{Cu-f} : diameter of Cu nanofibres inside Nb nanotubes; d_{Cu-i} : width of Cu- i channels ($i = 0$ to 3 or 4); UTS: ultimate tensile strength at room temperature.

Cu wires). Because of the cyclic process, the Cu matrix exhibits a multiscale structure, as illustrated by Fig. 1. For the Cu/Nb wires, the Cu matrix is distributed into the “Cu-0” interfilamentary channels, the “Cu-1” channels embedding N nanofilaments, the “Cu-2” channels embedding N^2 nanofilaments, etc. For the Cu/Nb/Cu wires, there is an additional component in the Cu matrix: the “Cu-f” nanofibers inside the Nb nanotubes. Here, nanotubular Cu/Nb/Cu wires are compared to nanofilamentary Cu/Nb wires with same total diameter $d = 1.5$ mm: their microstructure characteristics are given in Table 1.

TEM experiments [4, 5] revealed that Nb nanofilaments and nanotubes are composed of nanograins (diameter in the 50–200 nm range) elongated along the wire axis with sharp $\langle 110 \rangle$ fibre texture. Each Nb nanofilaments, in the Cu/Nb wire, tend to a single-crystalline 1-dimensional structure.

A double texture with $\langle 111 \rangle$ and $\langle 200 \rangle$ orientations was observed in the multiscale Cu matrix, with different types of Cu channels:

i) the “fine” Cu channels with sub-micrometer width (Cu-0 and Cu-1 channels for the Cu/Nb wire; Cu-0 and Cu-f channels for the Cu/Nb/Cu wire) are composed of individual grains

between Cu-Nb interfaces. Cu-0 channels can be viewed as a nanocrystalline layer around Nb nanofilaments or nanotubes. In the Cu/Nb/Cu system, the Cu-f nanofibres tend to a single-crystalline 1-dimensional structure.

ii) the “large” Cu channels with multi-micrometer width (Cu-2 to Cu-4 for the Cu/Nb wire; Cu-1 to Cu-3 for the Cu/Nb/Cu wire) are composed of grains from 200nm to the micrometer range with a high dislocation density and elongated along the wire axis.

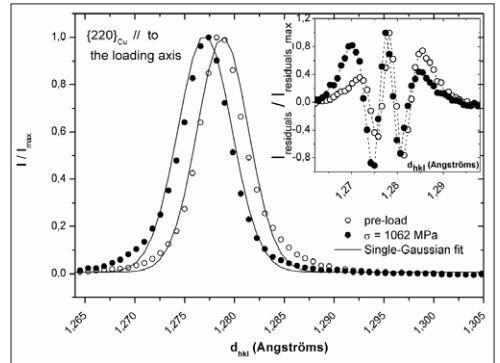


Figure 2: $(220)_{Cu}$ peak versus lattice spacing d_{hkl} at two stress levels (Cu/Nb wire), pre-load (\circ) and $\sigma=1062$ MPa (\bullet), for neutrons scattering onto planes that are parallel to the tensile axis: symbols correspond to raw data and lines to single Gaussian fits. Inset: residuals (i.e. difference between raw data and fit) versus d_{hkl} . From [7].

IN-SITU EXPERIMENTS

Neutron diffraction is performed during uniaxial tensile loading at room temperature at POLDI, a time-of-flight-diffractometer with multiple pulse overlap at the Swiss spallation neutron source SINQ (Paul Scherrer Institut, Switzerland) [6]. Diffraction is recorded from crystallographic planes parallel or perpendicular to the tensile axis, allowing measuring respectively the transverse and axial lattice strains. *Here the analysis is focused on the transverse strains.* Before measuring at a given applied strain, the sample was held 15 min at constant strain in order to allow relaxation [7]. In agreement with previously described textures, the most intense Cu peak, $(220)_{\text{Cu}}$, corresponds to grains that are either $\langle 111 \rangle$ or $\langle 200 \rangle$ textured along the wire axis. For the niobium, the most intense $(110)_{\text{Nb}}$ peak arises from the strong $\langle 110 \rangle_{\text{Nb}}$ axial texture.

Gaussian fits were used to determine peak positions, with errors smaller than 10^{-4}\AA . All (hkl) peaks were well fitted with a single Gaussian function, except the $(220)_{\text{Cu}}$ peak in transverse configuration. Fig. 2 shows, in the case of the Cu/Nb wire and for neutrons scattering on planes parallel to the tensile axis, the $(220)_{\text{Cu}}$ peak versus lattice spacing at two stress levels, pre-load ($\sigma=31\text{ MPa}$) and $\sigma=1062\text{ MPa}$. A strong peak asymmetry is observed at the high- d_{hkl} side for small stress and at the low- d_{hkl} side for high stress, this asymmetry changing gradually upon loading. This is more visible when plotting the difference between raw data and fit, i.e. the residuals displayed in inset of Fig. 2. This behavior was demonstrated to be the result of the superposition of two peaks, the first coming

from the large-Cu channels (intense and narrow peak), the second coming from the fine-Cu channels (less intense and broader peak related to the Cu nanochannels), as illustrated in inset of Fig. 3 [7].

Fig. 3 presents the evolution of the transverse elastic lattice strains in each phase versus applied stress for the Cu/Nb wire, the strain being calculated here as $(d_{\text{hkl}} - d_{\text{hkl}}^0)/d_{\text{hkl}}^0$, where d_{hkl}^0 and d_{hkl} are respectively the peak position in the pre-load state and the peak position in loaded state. From the evolution of the lattice strains in the large-Cu channels, in the fine-Cu channels and in the Nb nanofilaments, the co-deformation behaviour of the Cu/Nb wire can be uncovered: the large-Cu channels are the first to plastify at an applied stress around 500 MPa (deviation of elastic strain from linearity), then the fine-Cu channels yield at a stress close to 900 MPa. The fact that the elastic strain in the Nb nanofilaments does not stabilize shows that they remain in the elastic regime up to macro-

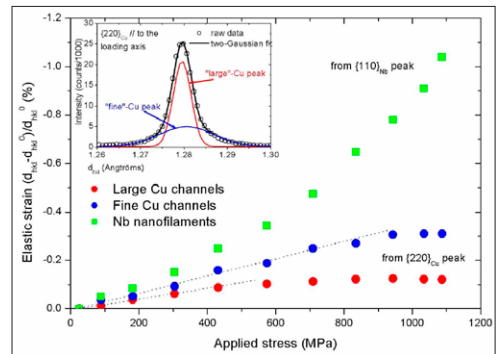


Figure 3: Evolution of transverse elastic strain versus applied stress in Cu and Nb phases in the Cu/Nb wire. Inset: example of the two-Gaussian decomposition of the $(220)_{\text{Cu}}$ diffraction peak in the pre-load state.

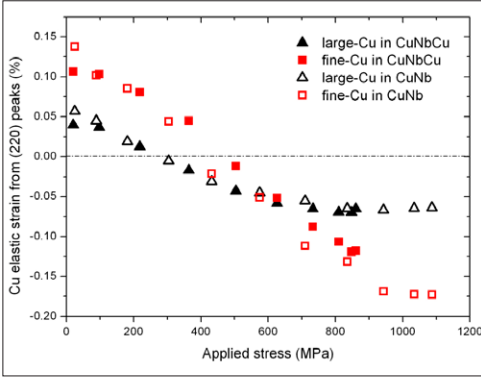


Figure 4: Evolution of Cu transverse elastic strains versus applied tensile stress calculated from $(220)_{\text{Cu}}$ peaks positions with stress-free state as reference, for large- and fine-Cu channels in the Cu/Nb/Cu ($d_{\text{Cu-0}} = 277$ nm, $d_{\text{Cu-f}} = 388$ nm) and the Cu/Nb ($d_{\text{Cu-0}} = 45$ nm, $d_{\text{Cu-1}} = 149$ nm) wires described in Table 1.

scopic failure of the wire: they behave as nanowhiskers with ultra high elastic limit. Moreover, the increasing rate of elastic strain in Nb is characteristic of a strong load transfer from the plastifying Cu matrix onto the elastic nanofilaments [7].

Fig. 4 compares the Cu transverse elastic strains calculated from the (220) peaks for the large- and fine-Cu channels as a function of applied stress for the Cu/Nb/Cu and the Cu/Nb wires: this time the strain is calculated with stress-free state as a reference ($d_{220}(\text{stress-free Cu}) = 1.278 \text{ \AA}$). For both wires, the transverse strain is first positive and then becomes negative with increasing applied stress: the Cu matrix is first in axial compression and is gradually unloaded and finally put into tension during tensile loading. This observation is in agreement with results obtained during load-unload experiments under synchrotron radiation, showing a strong Bauschinger effect in

the Cu matrix because the Cu matrix is put back into compression upon unloading [8]. The large-Cu channels behave similarly in the two types of wires: in the two samples, these Cu channels are indeed in the same cold worked state and have a similar ultra fine grain microstructure. In both wires, the fine-Cu channels exhibit an extended elastic regime compared to the large-Cu channels evidencing enhanced strengthening due to size effect. This is rather surprising for the Cu/Nb/Cu wire since the fine-Cu channels are still in the upper range of the nanometer regime, i.e. $d_{\text{Cu-0}} = 263$ nm and $d_{\text{Cu-f}} = 388$ nm, compared to $d_{\text{Cu-0}} = 45$ nm and $d_{\text{Cu-1}} = 149$ nm in the Cu/Nb wire. The difference lies however in the presence of Cu nanofibres (Cu-f) inside the Nb nanotubes. The contribution of the different types of fine-Cu channels have been estimated with appropriate scaling laws (Orwan-type or whisker-type) [4]: for Cu-0 channels with $d_{\text{Cu-0}} = 45$ nm (Cu/Nb wire) the yield stress is 1100 MPa, while for $d_{\text{Cu-0}} = 263$ nm (Cu/Nb/Cu wire) the yield stress is of the order of 500 MPa. In the Cu/Nb/Cu wire, the Cu-f nanofibres can be considered as nanowhiskers; their yield stress is estimated to 1.6 GPa [4]. These values show that the Cu nanofibres are the main contributor to the observed strengthening in the fine-Cu channels of the Cu/Nb/Cu wire.

Fig. 5 is a plot of the Nb transverse elastic strain calculated from the $(110)_{\text{Nb}}$ peaks versus applied stress for the Cu/Nb/Cu and the Cu/Nb wires (the strain is calculated with stress-free state as a reference, $d_{110}(\text{stress-free Nb}) = 2.333 \text{ \AA}$). In both systems, the Nb is initially in axial tension (negative transverse strain) and the absolute value of the elastic

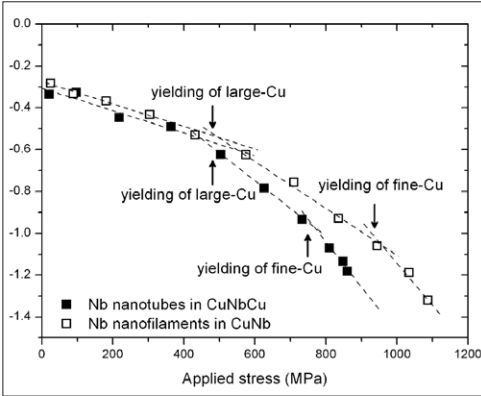


Figure 5: Evolution of Nb (110) transverse elastic strain versus applied tensile stress with stress-free state as reference for the Cu/Nb/Cu and Cu/Nb wires (Table 1).

strain increases continuously upon loading: the Nb nanotubes and nanofilaments remain in the elastic regime up to the wire fracture, in accordance with the yield stress enhancement of the Nb nanotubes due to an Orowan-type behaviour in the Cu/Nb/Cu system (Nb nanotubes) and a whisker-like behaviour in the Cu/Nb system (Nb nanofilaments) [3–5]. Again, a progressive load transfer onto the Nb occurs from the plastifying Cu matrix and can be correlated to the yielding of the different Cu channels: in the Cu/Nb/Cu system, this effect is more pronounced since the Nb content is lower and there is an earlier yielding of the fine-Cu channels.

CONCLUSIONS

In-situ deformation under neutrons allowed for detailed insight into the contributions of the different phases to the global deformation properties of multiscale nanocomposite Cu-Nb-based wires: initially, with increasing stress, both Cu and Nb phases are deforming elasti-

cally until the coarse Cu channels yield. At this stage, the Cu nanochannels as well as the Nb nanostructures (nanofilaments or nanotubes) are still deforming elastically, evidencing size effects that are correlated to the microstructure dimensions. Once the whole Cu matrix is in the plastic regime, a strong load transfer is observed onto the Nb that continues to deform elastically up to macroscopic fracture. When comparing Cu/Nb and Cu/Nb/Cu wires, the results suggest that a more efficient reinforcement can be obtained by designing different geometries, i.e. embedding Cu nanowhiskers in Nb nanotubes.

ACKNOWLEDGEMENT

This research project has been supported by the European Commission under the 6th Framework Programme through the Key Action: Strengthening the European Research Area, Research Infrastructures. Contract n°: RII3-CT-2003-505925.

REFERENCES

- [1] K.S. Kumar, H. Van Swygenhoven, S. Suresh, *Acta Mat.*, **51**, 5743 (2003)
- [2] K.Spencer, F. Lecouturier, L. Thilly, J.D. Embury, *Adv. Eng. Mat.*, **6**, 290 (2004)
- [3] L. Thilly, F. Lecouturier, J. Von Stebut, *Acta Mat.*, **50**, 5049 (2002)
- [4] V. Vidal, L. Thilly, F. Lecouturier, P.-O Renault, *Scripta Mater.*, **57**, 245 (2007)
- [5] L. Thilly, O. Ludwig, M. Véron, F. Lecouturier, J.P. Peyrade, S. Askénazy, *Phil. Mag. A*, **82**, 925 (2002)
- [6] U. Stuhr, M. Grosse, W. Wagner, *Mater. Sci. Eng. A*, **437**, 134 (2006)
- [7] L. Thilly, V. Vidal, S. Van Petegem, U. Stuhr, F. Lecouturier, P.-O. Renault, H. Van Swygenhoven, *Appl. Phys. Lett.*, **88**, 191906 (2006)
- [8] L. Thilly, S. Van Petegem, P.O. Renault, V. Vidal, F. Lecouturier, B. Schmitt, H. Van Swygenhoven, *Appl. Phys. Lett.*, **90**, 241907 (2007)

Neutron Scattering Spectroscopy of Relaxor Ferroelectrics

S. N. Gvasaliya¹, B. Roessli¹, G.M. Rotaru¹, R. A. Cowley², S. Kojima³, S. G. Lushnikov⁴, P. Günter⁵

¹Laboratory for Neutron Scattering, ETH Zurich and Paul Scherrer Institut, Villigen PSI, Switzerland

²Clarendon Laboratory, Oxford University, Parks Road, Oxford, UK

³Institute of Material Science, University of Tsukuba, Japan

⁴Ioffe Physico-Technical Institute RAS, St.-Petersburg

⁵Nonlinear Optics Laboratory, ETH-Hönggerberg, Zurich, Switzerland

INTRODUCTION

The relaxor ferroelectrics (shortly-relaxors) have been known for over 50 years but their properties are not yet understood and continue to be the subject of many experiments and theoretical considerations [1, 2]. They have a frequency-dependent peak in the dielectric permittivity ϵ' which typically extends over hundreds of degrees and is not necessarily related to a conventional ferroelectric phase transition. Since many physical properties of relaxors exhibit anomalies in this temperature range, the properties were called a "diffuse phase transition". Despite the large number of experimental studies of the phonons no evidence was found for soft mode in these materials. By using improved energy

resolution we have identified the soft mode as quasi-elastic scattering with an energy width of only about 0.5 meV while the transition is a random-field transition to a state having only short-range order and not the long-range order as in conventional ferroelectrics.

Relaxor ferroelectrics crystallize in different structures, but most of the efforts have been concentrated on the materials which have the relatively simple cubic perovskite-type structure in the paraelectric phase (space group Pm3m). Representative crystals are $\text{PbMg}_{1/3}\text{Nb}_{2/3}\text{O}_3$ (PMN), $\text{PbZn}_{1/3}\text{Nb}_{2/3}\text{O}_3$ (PZN), $\text{PbMg}_{1/3}\text{Ta}_{2/3}\text{O}_3$ (PMT), and these materials doped with PbTiO_3 (PT) [1]. The real part of the dielectric permittivity taken at the frequency 1 kHz is peaked at $T \sim 180$ K for PMT,

at $T \sim 270$ K for PMN, and at $T \sim 360$ K for PZN. PMT has a cubic structure. PMN is also cubic in the absence of an applied electric field down to the lowest temperature, but if an electric field above a threshold value is applied then a structural phase transition is induced below ~ 210 K. PZN undergoes a structural phase transition to a rhombohedral phase at $T_c \sim 365$ K. The x - T phase diagrams of the $(1-x)$ $\text{PbB}'_{1/3}\text{B}''_{2/3}\text{O}_3$ - $x\text{PbTiO}_3$ series are very rich as the doped materials undergo various phase transitions at lower temperatures. In certain compositional range ($x \sim 0.32$ for $(1-x)\text{PMN}$ - $x\text{PT}$ and $x \sim 0.07$ for $(1-x)\text{PZN}$ - $x\text{PT}$) the members of these series exhibit a large piezoelectric constant and a high dielectric permittivity and therefore they are widely used in industry.

All the crystals have an additional characteristic temperature, the Burns temperature – T_B . Most of the results suggest that above T_B the $(1-x)\text{PbB}'_{1/3}\text{B}''_{2/3}\text{O}_3$ - $x\text{PbTiO}_3$ materials behave similarly to conventional perovskite ferroelectrics. Below T_B the optical refractive index departs from the expected linear temperature dependence and this was explained by the appearance of small polar regions of the size of a few unit cells, which were referred to as ‘polar nano-regions’ (PNR) [3]. The values of T_B are 570, 620, 720 K for PMT, PMN, and PZN, respectively [4].

Since the $\text{PbB}'_{1/3}\text{B}''_{2/3}\text{O}_3$ crystals have the perovskite-like structure, it was expected that a soft transverse optic phonon would be observed and would give rise to the dielectric anomaly. An extensive search for the soft mode in these crystals with the main focus on PMN was performed both by light and neutron scattering (for a review see Refs. [5] and [6] correspondingly), but the soft mode was

not clearly observed. Here we describe our high-resolution neutron scattering experiments in the above mentioned crystals performed on the three-axis spectrometer TASP [7] at SINQ [8]. They show the soft mode of the transition is at lower frequencies than expected and occurs as dynamic quasi-elastic scattering in a random field as studied in detail for magnetic systems [9] and suggested to apply to relaxors. We start from the results obtained in studying the phase transition of PMN. After that we turn to the results obtained in the mixed materials with compositions close to the morphotropic phase boundary, namely the 0.68PMN-0.32PT and 0.93PZN-0.07PT. The experimental details and the procedure of the data treatment are given elsewhere [10–13].

LOW-ENERGY TRANSVERSE PHONONS

In ferroelectrics the transverse optic (TO) modes are expected to be the soft modes and consequently there have been many studies of the transverse phonons in relaxors. Our results were obtained by measuring the scattering with good experimental resolution near the $(2,2,0)$ Bragg reflection and then fitting a model whose parameters were constrained by symmetry and the model was convoluted with the experimental resolution. The results are qualitatively similar to those obtained by others and have interesting aspects such as a waterfall effect [6]. These results have not enabled the identification of the soft TO mode in relaxors.

Nevertheless in Fig.1 we show the intensity near the $(2,2,0)$ Bragg peak as calculated from the model. In addition to the transverse phonons there are two components of the

elastic scattering, mainly the strictly elastic component and a quasi-elastic component. However, systematic studies of the elastic scattering around the (2,2,0) Bragg peak are very difficult because there are two components of the diffuse scattering that must be distinguished from the transverse acoustic and TO phonon scattering and from the very strong (220) Bragg scattering. Due to the fact that at smaller Q the intensity of the TO is much reduced and that the kinematic conditions allow for a better energy resolution we have concentrated our studies of the properties of the diffuse scattering in the (1,1,0) Brillouin zone.

QUASIELASTIC AND CENTRAL PEAK SCATTERING IN PMN

Figure 2 shows the scattering obtained from PMN for $Q=(1,1,0.05)$ at three different temperatures, 670 K above the Burns temperature of 620 K, 430 K well below the Burns temperature and 300 K is an even lower temperature. The solid lines are fits to the spectra and the red lines are the scattering from the fits that cannot be described by resolution-limited elastic scattering (central peak scattering – CP) and result from the dynamic quasi-elastic scattering (QE). The spectrum at $T = 670$ K has a small strictly elastic component and no QE scattering. The strictly elastic scattering at this temperature arises from the incoherent scattering and from the B-site disorder of the Mg and Nb ions. At a temperature of 430 K the strictly elastic scattering has increased by a factor of less than 2 while there is a large and distinct quasi-elastic component. At lower temperatures the QE scattering is about the same intensity but the

strictly elastic CP scattering has increased by about a factor of 20. The susceptibility of the QE is represented by a Lorentzian shape in wavevector and energy [10, 11]:

$$\chi_{QE}(\mathbf{q}, \omega) = \frac{\chi(0, T)}{1 + q^2 \xi^2} \left(1 - i \frac{\omega}{\Gamma_q} \right)^{-1} \quad (1)$$

where ξ is the correlation length associated with the QE scattering and $\Gamma_q = \Gamma_0 + Dq^2$. The strictly elastic central peak is described by the scattering function: $S_{CP} = A(\mathbf{Q})\delta(\omega)$ (2)

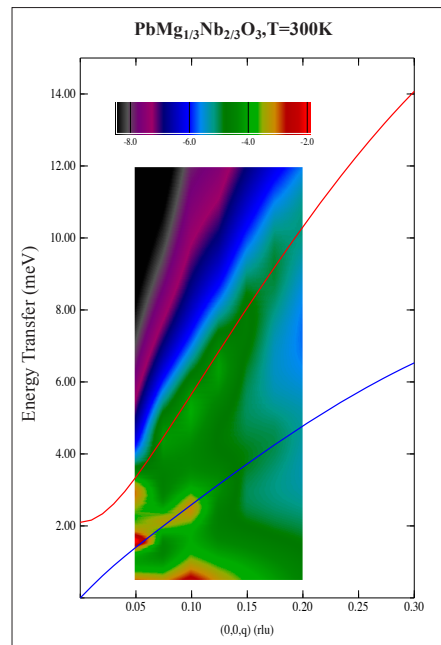


Fig. 1: Calculated colour map from the model parameters of the distribution of the intensity around the (220) Bragg peak of PMN at $T=300$ K. The blue (red) line shows the dispersion of the TA (TO) phonons. The intensity is given in a logarithmic scale. $1 \text{ r.l.u.} = 1.555 \text{ \AA}^{-1}$. Note a significant intensity close to zero energy transfer.

These expressions and those for the phonons were convoluted with the experimental resolution and then fitted to the experimental results. Initially we consider the temperature dependence of the quasi-elastic scattering. The susceptibility of the QE scattering in PMN is shown in Fig. 3. It increases on cooling below 600 K reaching a maximum at about 370 K and then decreases on further cooling. The temperature dependence of the $\chi_{QE}(0, T)$ is similar to the real part of the dielectric permittivity ϵ' when taken at sufficiently high frequencies. The frequency width of the QE scattering is shown in Fig. 4 as deduced from the measurements at $Q = (1, 1, 0.05)$. The linewidth of the QE scattering decreases with decreasing temperature from about 0.5 meV at 600 K to 0.1 meV at 200 K.

Thus, the QE scattering appears below the Burns temperature T_B and the susceptibility of the QE scattering peaks around $T_m \sim 370$ K. The characteristic energy width of the fluctuations associated with the QE scattering decreases. Such a behavior is consistent with a phase transition at T_m . This conclusion is also supported by the anomaly in the specific heat of PMN occurring close to T_m [14].

However this phase transition is not a conventional phase transition to a long range ordered state. The correlation ξ associated with the QE scattering does not diverge at T_m , but continuously increases towards T_m and saturates below this temperature at $\sim 11\text{\AA}$. Furthermore, there is no onset of long-range ferroelectric order below T_m as shown by the elastic scattering in Fig. 5. The intensity of the elastic CP scattering indeed increases drastically below T_m , but it never turns into the Bragg peak scattering as clearly seen in the

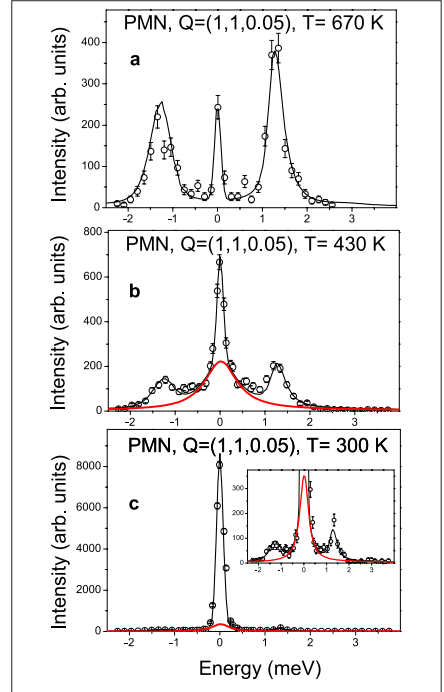


Fig. 2: Constant- Q scans from PMN at 3 temperatures. The black solid line is the fit to the model and the red line is the quasi-elastic component.

right panel of Fig. 5. The HWHM of the CP scattering decreases gradually from 0.04 rlu at 400 K to 0.015 rlu at 150 K, while the best fit of the CP lineshape is achieved with a Lorentzian function raised to the power of 1.5 and that is shown by the red line in Fig. 5.

This behavior of PMN is consistent with a random field transition occurring at about 370 K as the sample was field-cooled in the random fields produced by the PNR. The order parameter does not have long range order but has a line-shape in q given by a Lorentzian raised to a power more than 1, as observed

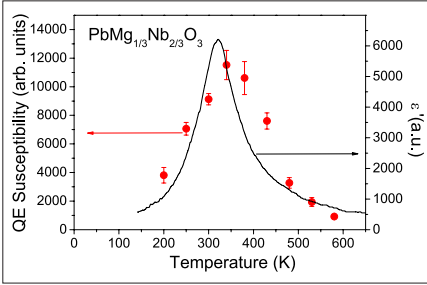


Fig. 3: Temperature dependence of the susceptibility of the QE scattering in PMN (red circles). For comparison the real part of the dielectric permittivity of PMN at frequency 1 GHz is also shown (dielectric data is from Ref. [15]).

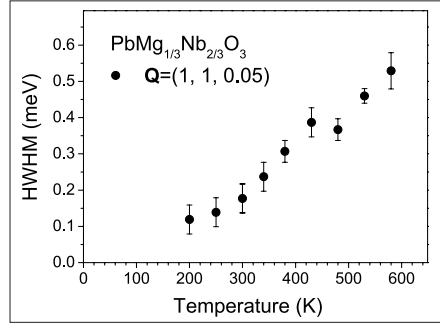


Fig. 4: Temperature dependence of the half-width at the half-maximum of the QE scattering in PMN measured at $Q=(1, 1, 0.05)$.

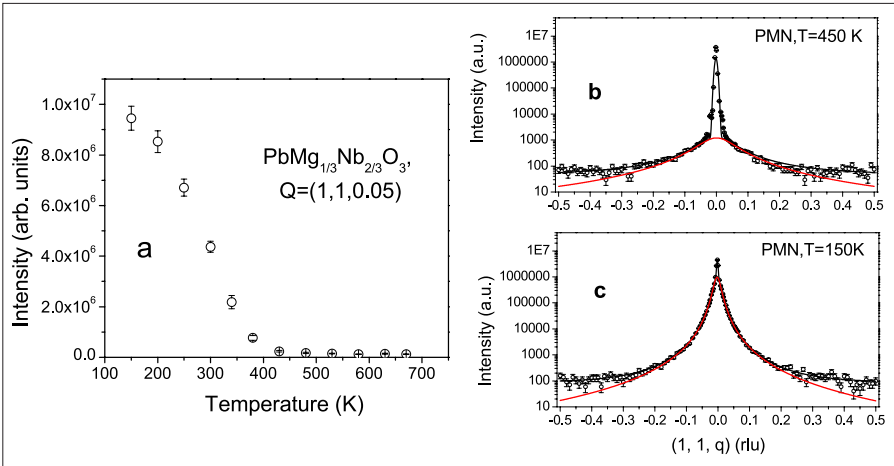


Fig. 5: Evolution of strictly elastic diffuse scattering in $\text{PbMg}_{1/3}\text{Nb}_{2/3}\text{O}_3$. (left) Temperature dependence of the intensity of the strictly elastic central peak taken at $Q=(1, 1, 0.05)$. (right) Elastic transverse scans in the vicinity of the $(1, 1, 0)$ Bragg peak at two selected temperatures.

at magnetic transitions in random fields [9]. The correlation length for the dynamic scattering is not infinite at the transition temperature as commonly observed at long-range magnetic transitions. Unfortunately it is not possible to zero-field cool the systems as is done for diluted antiferromagnets in an applied field.

QUASIELASTIC AND CENTRAL PEAK SCATTERING IN PMN-PT AND PZN-PT

The properties of the two components of the diffuse scattering were studied in the 0.68PMN-0.32PT and in the 0.93PZN-0.07PT crystals through the phase transitions. The results are very similar for the two materials. The high-resolution neutron spectra from the 0.68PMN-0.32PT can be found in Ref. [12] and spectra at two temperatures from the 0.93PZN-0.07PT with the wavevector $Q=(1,1,0.075)$ are given in Fig. 6. The spectrum shown in Fig. 6a is measured somewhat below the Burns temperature of 0.93PZN-0.07PT, while the spectrum given in Fig. 6b is taken close to the ferroelectric phase transition. The solid lines are fits to the spectra according to the model [13] and the red solid lines emphasize the contribution of the dynamic QE scattering. The spectrum at $T = 630$ K has a small strictly elastic CP component and a pronounced broad quasi-elastic component (note that the incoherent scattering is removed from the spectra of 0.93PZN-0.07PT). Close to the phase transition the most significant changes in the spectrum are the increase of the intensity of the strictly elastic CP and the change in the intensity and width of the QE scattering. Very similar behavior of the spectra from the 0.68PMN-0.32PT crystal was observed in Ref. [12].

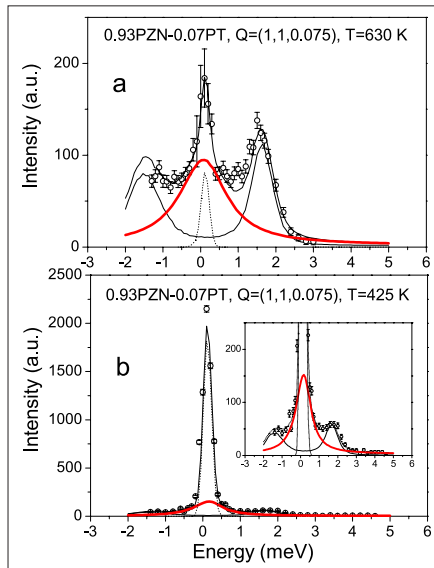


Fig. 6: Typical const- Q scans at $T=630$ K (a) and at $T=425$ K (b). The solid line is the fit to the model. The bold red line emphasizes the contribution of the QE component. The dotted line shows the strictly elastic CP scattering. The incoherent scattering was measured at high temperature away from the $(1,1,0)$ Bragg peak and subtracted from the data.

The temperature dependences of the parameters of the QE and of the CP scattering are essentially similar in 0.68PMN-0.32PT and in 0.93PZN-0.07PT. Figure 7 shows the temperature dependences of the susceptibility of the QE scattering and of the dielectric permittivity. The susceptibility of the QE scattering follows the temperature dependence of the real part of dielectric permittivity. The results were similar for the 0.68PMN-0.32PT [12]. Note that in both mixed materials the dielectric permittivity was almost independent of the frequency of the measurements unlike the behavior in pure PMN.

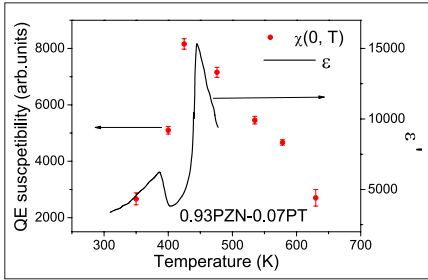


Fig. 7: Temperature dependence of the susceptibility of the QE scattering in the 0.93PZN-0.07PT (red circles). For comparison the real part of the dielectric permittivity of 0.93PZN-0.07PT is also shown (dielectric data is from Ref. [16]).

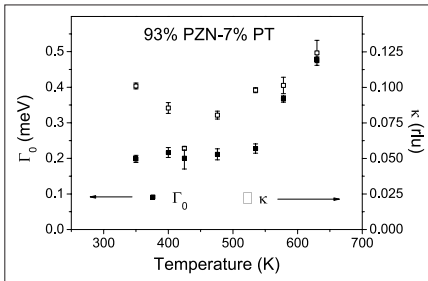


Fig. 8: Temperature dependences of the damping of the QE scattering Γ_0 and of the inverse correlation length κ in the 0.93PZN-0.07PT.

Figure 8 shows the temperature dependence of the damping and of the inverse correlation length associated with the QE scattering in 0.93PZN-0.07PT. Both have minima at the transition as expected for an antiferromagnetic long-range transition. The intensity of the CP scattering has a weak maximum at about the same temperature [13]. Similar behavior is found in 0.68PMN-0.32PT.

DISCUSSION AND CONCLUSIONS

We have made high resolution neutron scattering experiments in some of the relaxor ferroelectrics. High resolution both in energy and wavevector is essential to distinguish between the components of the scattering, especially close to the Bragg peaks. The experiments suggest that below the Burns temperature of each material there appear dynamic polar nano-regions that give rise to the QE scattering. In all cases studied so far the susceptibility of the QE scattering is similar to the temperature dependence of the dielectric permittivity ϵ' . This suggests that the dielectric anomaly and the QE scattering are due to the same dynamic correlations that produce the PNR. As the temperature decreases, the dynamic PNR tend to freeze and become static PNR giving rise to the strictly elastic CP scattering. This occurs at a random-field phase transition which does not establish long-range ferroelectric order as observed in PMN. In the mixed materials PMN-PT and PZN-PT the PNR align in one direction and there is a transition to a long-range ordered phase. This may occur when the PNR freeze. Alternatively at a lower temperature below the random-field transition there may be a long-range ferroelectric transition. These possibilities depend on the strength of the random fields and the ferroelectric fluctuations.

In conclusion we have identified the soft modes in relaxor ferroelectrics. They occur at lower energy transfers than expected ~ 0.5 meV and can only be studied in detail with high-resolution neutron scattering. We have shown that the transition in relaxors can be to a state without a long range order due to the randomly oriented PNR's and is similar to

the random field transition observed in diluted antiferromagnets in an applied field.

ACKNOWLEDGMENTS

This work was performed at the Swiss spallation neutron source SINQ, Paul Scherrer Institut, and was partially supported by the Swiss National Foundation (Project No. 20002-111545) and by the Leverhulme foundation.

REFERENCES

- [1] G.A. Smolenskii et al., *Ferroelectrics and Related Materials* (Gordon and Breach, New York, 1984).
- [2] V. Westphal, W. Kleemann, and M.D. Glinchuk, *Phys. Rev. Lett.* **68**, 847 (1992); D. Viehland, S.J. Jang, L.E. Cross, and M. Wuttig, *Phys. Rev. B* **46**, 8003 (1992); R. Blinc, J. Dolinsek, A. Gregorovic, B. Zalar, C. Filipic, Z. Kutnjak, A. Levstik, and R. Pirc, *Phys. Rev. Lett.* **83**, 424 (1999).
- [3] G. Burns and B.A. Scott, *Solid State Commun.* **13**, 423 (1973).
- [4] O.Y. Korshunov, P. A. Markovin, and R. V. Pisarev, *Ferroelectr., Lett. Sect.* **13**, 137 (1992).
- [5] I.G. Siny, S.G. Lushnikov, R.S. Kariyar, and V.H. Schmidt, *Ferroelectrics* **226**, 191 (1997).
- [6] C. Stock, H. Luo, D. Viehland, J.F. Li, I.P. Swainson, R.J. Birgeneau and G. Shirane, *J. Phys. Soc. Jpn.* **74**, 3002 (2005); K. Hirota, S. Wakimoto, D.E. Cox, *J. Phys. Soc. Jpn.* **75**, 111006 (2006).
- [7] F. Semadeni, B. Roessli, and P. Boni, *Physica B* **297**, 152 (2001).
- [8] W.E. Fischer, *Physica B* **234&236**, 1202 (1997).
- [9] H. Yoshizawa, R.A. Cowley, G. Shirane, and R.J. Birgeneau, H. Ikeda, *Phys. Rev. Lett.* **48**, 438 (1982); R.A. Cowley, G. Shirane, H. Yoshizawa, Y.G. Uemura, and R.J. Birgeneau, *Z. Phys. B* **75**, 303 (1989).
- [10] S. N. Gvasaliya, S.G. Lushnikov and B. Roessli, *Phys. Rev. B* **69**, 092105 (2004).
- [11] S.N. Gvasaliya, B. Roessli, R.A. Cowley, P. Huber, and S.G. Lushnikov, *J. Phys.: Condens. Matter* **17**, 4343 (2005).
- [12] S.N. Gvasaliya, B. Roessli, R.A. Cowley, S. Kojima, and S.G. Lushnikov, *J. Phys.: Condens. Matter* **19**, 016219 (2007).
- [13] G.-M. Rotaru, S.N. Gvasaliya, B. Roessli, S. Kojima, S.G. Lushnikov, P. Guenter, *Appl. Phys. Lett.* **93**, (2008); cond-mat > arXiv:0805.2908 (2008).
- [14] Y. Moriya, H. Kawaji, T. Tojo, T. Atake, *Phys. Rev. Lett.* **90**, 205901 (2003).
- [15] V. Bovtun, et al., *Ferroelectrics* **298** (2004) 23.
- [16] Y. Hosono, et al., *Jpn. J. Appl. Phys.* **41**, 7084 (2002).

The First “joint X+N” Proposals Round for Powder Diffraction Experiments at PSI

D. Cheptyakov¹, W. Pomjakushin¹, P. Willmott², F. Gozzo²

¹ Laboratory for Neutron Scattering, Paul Scherrer Institut & ETH Zürich, 5232 Villigen PSI, Switzerland

² Laboratory for Synchrotron Radiation, Paul Scherrer Institut, 5232 Villigen PSI, Switzerland

Operating several large scale facilities at one location has allowed the Paul Scherrer Institut in Villigen to launch a new mode of accessing multiple instruments with a unique beamtime application. In an initial trial period, the obvious complementarity of neutron and X-ray powder diffraction methods for crystal structure analysis in established fields of neutron and X-ray diffraction applications (e.g. crystallography, magnetism, materials science) has been exploited. It is a generally accepted approach to use both probes in order to obtain the whole picture for structural solutions. Therefore, instead of expecting the users to submit separate proposals for the different facilities (often situated in different countries), SINQ and SLS have created a new, independent channel of access – through a single proposal submission justifying the need for both probes. Such an option not only makes the access to the world-class large scale facilities of PSI much easier and faster for the users, but also generates a positive effect of

the overall scientific profile of the work performed at both the neutron source SINQ and the SLS synchrotron.

A certain amount of time was reserved at the high-resolution powder diffractometer HRPT at SINQ and the powder diffraction station of the Materials Sciences Beamline at the SLS. The non-coincidence of the proposal submission deadlines for the two facilities has been overcome by defining a separate new deadline preceding both the SINQ and SLS deadlines and by processing the major part of the usual paperwork electronically. The SINQ Scientific Advisory Committee (SAC) and both the SLS Peer Review Committee (PRC) and the SLS-SAC in their meetings in summer 2007 welcomed the idea of carrying out this “joint X+N” proposals Round, and many members kindly agreed to act as reviewers of these “joint” proposals.

Only users that were already registered for the diffraction instruments of SINQ and SLS were explicitly invited to take the opportu-

nity of this first trial Round, and we have received a very satisfactory response. As a result of the first proposals review, the best seven projects have been accepted. The experiments have already been scheduled and will be carried out in June-November 2008. Almost all the "joint X+N" users will have to come only once to PSI for carrying out their experiments at both facilities.

We are looking forward to the evaluation of its results, which is expected to follow in the late 2008 or early 2009. We hope the initiative will be supported by the results and a decision will be taken to continue and may be expand the "Joint" Proposals Rounds to other PSI facilities.

Walter E. Fischer (1939 – 2008)

A. Furrer

Laboratory for Neutron Scattering, Paul Scherrer Institut & ETH Zürich, 5232 Villigen PSI, Switzerland

Walter Fischer, the pioneer in establishing the spallation neutron source SINQ at PSI Villigen, passed away on March 17, 2008, after half a year's battle with cancer. In spite of his illness, he has been active at PSI until February 2008, finishing his book "NEUTRONS, X-RAYS and MUONS – The theoretical principles of their applications in solid state physics". His book will be a highly respected memory for all his friends and colleagues in the future.

Walter studied theoretical physics at the ETH Zurich where he received his masters degree in the year 1964 with a work on "monoenergetic positrons and internal pair creation". Three years later he graduated from the ETH Zurich with theoretical studies in "meson spectroscopy", a work which was carried out at the CERN in Geneva. In 1968 he joined the theory group of the former Swiss Institute for Nuclear Research (SIN Villigen). His task was to prepare the basis for future experiments at the SIN meson facility, and his work focused on the interplay between weak, strong and electromagnetic interactions. During this time he developed an increasing interest in solid state physics, particularly in muon experiments which became feasible at SIN. In 1972 he spent some time at the JINR Dubna in order to deepen his knowledge in this field. Upon returning to SIN he was one of the

organizers of the "Bürgenstock Meeting" where the techniques of muon spin rotation, relaxation and resonance were successfully advertised to a wider scientific community.

In 1974 Walter joined the accelerator division of SIN where he was involved in methods of beam development and operation. In particular, he was in charge of the design study to inject 860 keV protons into today's injector system which was a serious problem due to space charge considerations. He also started to think about a possible parasitic use of the intense "waste beam" of the SIN accelerator which – after passing through some meson targets – was just directed to a beam dump without any further use. That's when the first ideas came up to use the waste beam for a spallation neutron source. Walter got deeply involved into this fascinating idea which he pushed forward as a visionary project with great enthusiasm. In 1978 he came up with a project proposal and called a meeting at Villigen to present the case of the spallation neutron source SINQ which was unanimously welcomed by the Swiss condensed matter community. About two decades later Walter's vision became reality!

Immediately after this meeting the director of SIN appointed Walter as SINQ project leader and head of the SINQ project group.

An intense phase of international collaboration began. Together with experts from Julich, Karlsruhe, and Munich a mock-up experiment was installed at the SIN accelerator to demonstrate experimentally the expected performance of SINQ. In addition, calorimetric measurements were performed at the accelerator in Vancouver to test the properties of some target materials as well as the cold source under intense proton irradiation. All these works set a reliable basis for the SINQ project which was then approved and funded by the Swiss Government and Parliament in 1986/87. In August 1988 the construction work of SINQ started, and Walter's responsibilities grew accordingly with the project group which became rather a project department. SINQ was a high-risk project, and many unexpected problems had to be solved during the construction phase. During that time Walter's permanent optimism and enthusiasm as well as his deep knowledge of all the technical details were essential for the success of the project. On December 3, 1996, SINQ produced the first neutrons with measured fluxes being in complete agreement with the expectations. Already in the second half of 1997 SINQ started user operation. In the last decade some three thousand users from all over the world performed experiments at SINQ which has become a powerful neutron source in Europe.

After the fusion of SIN with the former Swiss Federal Institute of Reactor Research (EIR Wurenlingen) to the Paul Scherrer Institute (PSI Villigen) in the year 1989, Walter moved upwards in the hierarchy. He was appointed deputy director of the Department "Solid State Physics at Large Facilities", and

one year later he became its director. He recognized that experimental work at SINQ has to be accompanied by theoretical work, thus he founded a "Condensed Matter Theory Group". After an internal reorganisation in 1999 he became the director of the newly established Department "Condensed Matter Research with Neutrons", a position which he held until his official retirement in 2004.

After the successful realization of SINQ, Walter had some spare time for scientific work – besides his administrative duties. He wrote comprehensive articles on the theoretical principles of neutron and synchrotron x-ray scattering which he presented to the participants of many schools and workshops in his captivating charm, thereby impressing and convincing people and getting them to listen carefully to his arguments. He was also the initiator of the Zuoz Neutron Schools which took place every summer from 1993 until 2000. Walter Fischer's activities, however, did not only touch scientific and technological topics associated with neutrons, but his background was extremely broad and covered disciplines such as astrophysics, geology, and history, which was actually the fundus of the many unforgettable, joking after-dinner speeches at the Zuoz Schools and at other occasions. I gratefully look back to many years of co-operation with Walter Fischer as a gentleman in every sense of the word – gentle, courteous, very considerate, firm in his convictions, and with a good sense of humour. Now we will sadly miss him, but we will never forget him.

Joël F. Mesot

New Director of the Paul Scherrer Institute

S. Janssen, K. N. Clausen
Paul Scherrer Institut, Department NUM



On December 21, 2007 the Swiss government appointed Joël F. Mesot as director of the Paul Scherrer Institute (PSI) in Villigen, Switzerland. With that vote the government followed the unanimous proposal of the selection committee and the board of the Swiss Federal Institutes. From August 1,

2008 on he will follow Martin Jermann, who lead the institute ad interim since summer 2007, when the former director Ralph Eichler was elected to chair the Swiss Federal Institute (ETH) in Zurich.

Joël Mesot (born 1964) is a solid-state physicist with special emphasis on materials with new electronic properties. He has an outstanding scientific reputation and record in particular in the fields of high-temperature superconductors and is a well-known expert both in neutron scattering and photoelectron spectroscopy. In 2002 he was awarded the prestigious Latsis Prize of the ETH Zurich for his scientific achievements.

As a Swiss he studied physics at ETH Zurich and performed his PhD at the ILL Grenoble. He then returned to the Laboratory for Neutron Scattering (LNS) of the PSI and the ETH Zurich and after a stay as Postdoctoral Fellow at Argonne National Laboratory (IL, USA) he became head of the spectroscopy group of the laboratory. In December 2004 he was appointed as director of the LNS. He is titular professor at ETH Zurich and since 2007 also head of the PSI research commission. Between 2003 and 2007 he was chief editor of the "Neutron News Journal" as successor of Gerry Lander.

PSI is the largest national research centre in Switzerland and is active in solid state physics, materials sciences, elementary particle physics, life sciences, nuclear and non-nuclear energy research, and energy-related ecology. With 1300 members of staff it hosts the three major user laboratories SLS (X-ray synchrotron), SINQ (spallation neutron source) and SμS (Swiss muon source) with approximately 1800 individual users per year.

Joël, your colleagues and friends wish you enthusiasm, good luck and all the best for your responsible new task!

SGN Financial Report 2007

The annual assembly 2008 of the Swiss Neutron Scattering Society will be organized on November 28, 2008 (see announcements within this issue). Since this is quite late in the year, the financial report 2007 and the audit 2007 are published already now:

Annual balance sheet 2007:

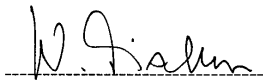
Assets SGN/SSDN on 1.1.2007: **CHF 5.539,85**

	Revenues [CHF]	Expenses [CHF]
Membership-fees (cash box)	90,00	
Membership-fees (postal check acc.)	585,21	
Donations (cash box)	–	
Total expenses		2.231,50
– Apéro Zuoz (2007)		712,70
– Apéro W. Hälgi Kolloquium		1.478,80
– Expenses PC account		40,20
Credit for accrued interest	2,35	
Total	677,56	2.231,50
Net earnings 2007:		-1.553,94
Assets SGN/SSDN on 31.12.07:		3.985,91

Balance sheet 2007:

	Assets [CHF]	Liabilities [CHF]
Postal check account	2.087,41	
Cash box	1.898,50	
Assets on 31.12.07	3.985,91	

Die Rechnungsrevisoren haben die Belege, die Abrechnungen und die Bilanz für das Jahr 2007 geprüft und für in Ordnung befunden!

8.12.07		24.1.08	
Datum	Dr. W. Fischer, PSI	Datum	Dr. K. Krämer, Uni Bern



7th PSI Summer School on Condensed Matter Research

August 16 –22, 2008

Probing the Nanometer Scale with Neutrons, Photons and Muons

The properties of a material may be dramatically altered either when one or more of its spatial **dimensions are reduced to the nanometer scale or within nanometer distances** from an interface to another material with very different properties. The latter proximity effect may lead to very **strong coupling between properties such as magnetism, resistivity, superconductivity, ferroelectricity**, etc. In this school we will show how **neutrons, synchrotron X-rays and muons** can be used to probe these materials and detect **new phenomena on the nm scale**. Various techniques based on the use of neutrons, muons and photons (powder diffraction, small angle scatter-

ing, reflectometry, muon spin rotation/relaxation, real space imaging and X-ray circular dichroism) will be introduced and **examples from the fields of superconductivity, magnetism, ferroelectricity, material science, food science and soft matter science** will be presented.

The school is addressed mainly to the education of PhD and postdoctoral students without prior knowledge of neutron, X-ray and muon techniques. It is fully open to the national and non-national public and the language of the school is English.

More information:

<http://num.web.psi.ch/zuoz2008/>

Announcements

SGN/SSDN Members

The Swiss Neutron Scattering Society welcomes the following new member:

Artur Braun, EMPA Dübendorf, Switzerland

Presently the SGN has 201 members. Online registration for new members of our society is available from the SGN website:

<http://sgn.web.psi.ch>

SGN/SSDN Annual General Assembly '08

The 2008 General Assembly of the Swiss Neutron Scattering Society will be organized on **November 28, 2008** at the Paul Scherrer Institut in Villigen. The Assembly will be a satellite meeting of a dedicated symposium on the occasion of the 20th anniversary of the Swiss ILL membership. Please reserve the date in your agendas already now. The invitations for the society members with a detailed agenda will follow in due time.

SGN/SSDN Annual Member Fee

The SGN/SSDN members are kindly asked to pay their member fees 2008 (if not already done). The annual member fee is still CHF 10,- and can be paid either by bank transfer or in cash during your next visit at PSI. The bank account of the society is accessible for both Swiss national and international bank transfers. The coordinates are as follows: Post-finance: 50-70723-6 (BIC: POFICHBE), IBAN: CH39 0900 0000 5007 0723 6

SINQ Call for Proposals

The next DEADLINE for the submission of beam time requests for the Swiss spallation neutron source "SINQ"

(<http://sinq.web.psi.ch>) will be:

November 15, 2008

Registration of Publications

You are kindly asked to register your SINQ/SLS/SμS related publications within the PSI Digital User Office DUO: <https://duo.psi.ch>. In particular we need the information about recent publications for the annual reports. Please use the link "publications" from the DUO main menu and follow the online instructions. The DUO publication tool is easy to use and self-explaining but please don't hesitate to contact us if anything remains unclear: sinq@psi.ch. You can use your DUO publication records as a reference in your new proposals.

Open Positions at ILL

To check the open positions at ILL please have a look at the following ILL-Webpage:

<http://www.ill.eu/careers>

Conferences and Workshops 2008

(an updated list with online links can be found here: <http://sinq.web.psi.ch/sinq/links.html>)

JULY

International School of Physics 'Enrico Fermi': Quantum Coherence in Solid State Systems

July 1–11, 2008, Varenna, Lake Como, Italy

SXNS 10: International Conference on Surface X-Ray and Neutron Scattering

July 2–5, 2008, LLB Saclay, France

ICL 08: 15th International Conference on Luminescence and Optical Spectroscopy of Condensed Matter

July 7–11, 2008, Lyon, France

50 Years of Neutron Science in Berlin

July 14–15, 2008, Berlin, Germany

ANSTO-AINSE Neutron School on Materials

July 20–25, 2008, Lucas Heights, Sydney, Australia

XRM 2008: 9th International Conference on X-Ray Microscopy

July 21–25, 2008, Zurich, Switzerland

μ SR 2008: 11th International Conference on Muon Spin Rotation, Relaxation, and Resonance

July 21–25, 2008, Tsukuba, Japan

5th LANSCE Neutron School: Magnetism in Bulk and Nanostructured Materials

July 23 – August 1, Los Alamos, USA

STRIPES 08: 6th International Conference of the 'Stripes and High-Tc Superconductivity' Series

July 26 – August 1, Erice, Sicily, Italy

AUGUST

LT25: 25th International Conference on Low Temperature Physics

August 6–13, 2008, Amsterdam, The Netherlands

7th PSI Summer School on Condensed Matter Research

August 16–22, 2008, Zuoz, Switzerland

1st Asia-Oceania Neutron Scattering Summer School

August 18–23, 2008, Daejeon, South Korea

IUCr Crystallographic Computing School 2008

August 18–23, 2008, Kyoto, Japan

IUCr 2008: XXI Congress of the International Union of Crystallography

August 23–31, 2008, Osaka, Japan

CMD22: 22nd General Conference of the Condensed Matter Division of the European Physical Society
August 25–29, 2008, Rome, Italy

SEPTEMBER

PNCMI2008/QuBS2008: 7th International Workshop on Polarized Neutrons in Condensed Matter Investigations
September 1–5, 2008, Tokai, Ibaraki, Japan

12th JCNS Laboratory Course – Neutron Scattering
September 1–12, 2008, Jülich and Garching, Germany

Noclams Workshop on New Opportunities and Challenges for Liquid and Amorphous Materials Science
September 3–5, 2008, ESRF, Grenoble, France

HFM2008: International Conference on Highly Frustrated Magnetism
September 7–12, 2008, Braunschweig, Germany

ISBB 2008: 16th International Symposium on Boron, Borides and Related Materials
September 7–12, 2008, Matsue, Shimane, Japan

6th NCCR Symposium on New Trends in Structural Biology
September 8–9, 2008, Zürich, Switzerland

German Neutron Scattering Conference
September 15–17, 2008, Garching, Germany

ICTMC-16: International Conference of Ternary and Multinary Compounds
September 15–19, 2008, Technical University of Berlin, Germany

Erasmus Mundus MaMaSelf Sommer School 2008
September 15–27, 2008, University of Rennes, France

Powder Diffraction Software Workshop
September 18, 2008, Warsaw, Poland

EPDIC-11: 11th European Powder Diffraction Conference, Satellite workshop to EPDIC 11
September 19–22, 2008, Warsaw, Poland

IXth School of Neutron Scattering “Francesco Paolo Ricci”: Applications of Neutrons to Structural Determination in Soft Matter
September 22 – October 3, 2008, Pula, Sardinia, Italy

Biomolecular Dynamics and Protein-Water Interactions

September 24–26, 2008, Feldafing/Munich, Germany

Workshop on Diffuse Scattering and Structure Simulation

September 24–26, 2008, Erlangen/Nürnberg, Germany

10th United States National School on Neutron and X-ray Scattering

September 24 – October 11, 2008, Argonne and Oak Ridge, USA

OCTOBER

JCNS Workshop on Modern Trends in Neutron Scattering Instrumentation

October 15–17, 2008, Munich, Germany

EMBO Practical Course on Solution Scattering from Biological Macromolecules

October 19–26, 2008, EMBL Hamburg, Germany

NOVEMBER

NOBUGS 2008

November 3–5, 2008, ANSTO, Sidney, Australia

2008 ISIS Molecular Spectroscopy User Group Meeting

November 4–5, 2008, Abingdon, United Kingdom

ICTF 14: 14th International Conference on Thin Films

November 17–20, 2008, Ghent, Belgium

Conferences and Workshops 2009

(an updated list with online links can be found here: <http://sinq.web.psi.ch/sinq/links.html>)

FEBRUARY

QENS 2009: 9th International Conference on Quasielastic Neutron Scattering
February 10–13, 2009, PSI Villigen, Switzerland

MAY

International Topical Meeting on Nuclear Research Applications and Utilization of Accelerators
May 4–8, 2009, Vienna, Austria

JUNE

ICC 14: XIV International Clay Conference
June 14–20, 2009, Castellaneta, Italy

ICNX 2009: International Conference on Neutron and X-Ray Scattering
June 22–24, 2009, Kuala Lumpur, Malaysia

AUGUST

ECM 25: 25th European Crystallographic Meeting
August 2009, Istanbul, Turkey

SEPTEMBER

SAS-2009: XIV International Conference on Small-Angle Scattering
September 13–18, 2009, Rutherford Appleton Laboratory, Oxford, United Kingdom

Swiss Neutron Scattering Society

Sekretariat SGN/SSDN

Paul Scherrer Institut

bldg. WLGA/018

5232 Villigen PSI, Switzerland